

# Cell Adhesion Mechanisms and Elasto-Viscoplastic Mechanics of Tumours

D. Ambrosi, L. Preziosi

Dipartimento di Matematica, Politecnico di Torino

Corso Duca degli Abruzzi 24, I-10129, Torino, Italy,

davide.ambrosi@polito.it - luigi.preziosi@polito.it

September 24, 2008

## Abstract

Tumour cells usually live in a environment formed by other host cells, extra-cellular matrix and extra-cellular liquid. Cells duplicate, reorganise and deform while binding each other thanks to adhesion molecules exerting forces of measurable strength. In this paper it is illustrated a macroscopic mechanical model of solid tumour which takes such adhesion mechanisms into account. The extracellular matrix is treated as an elastic compressible material, while, in order to define the relationship between stress and strain for the cellular constituents, the deformation gradient is decomposed in a multiplicative way distinguishing the contribution due to growth, to plastic rearrangement and to elastic deformation. On the basis of experimental results at a cellular level, it is proposed that at a macroscopic level there exists a yield condition separating the elastic and viscoplastic regimes. Previously proposed models are obtained as limit cases, e.g. fluid-like models are obtained in the limit of fast cell reorganisation and negligible yield stress. A numerical test case shows that the model is able to account for several complex interactions: how tumour growth can be influenced by stress, how and where it can generate plastic reorganisation of the cells, how it can lead to capsule formation and compression of the surrounding tissue.

## Introduction

Most research on solid tumour growth historically focuses on the interplay between the biochemical factors that promote or inhibit growth and angiogenesis. Mechanical effects have been neglected for a long time, until recent experiments have shown that they play a non-negligible role. As an example, Helmlinger *et al.* measured the diameter of growing cellular spheroids in gels of different rigidity and demonstrate that the tumour size depends on the normal load exerted by the surrounding gel on the multicellular spheroid [26].

The modelling literature devoted to such mechanisms has appeared just in recent years. In absence of extensive experimental data, several approaches have been proposed, based on a variety of assumptions, the main differences being summarised below.

1. The mechanical stress-strain constitutive equation. Most models use fluid-like constitutive equations [3, 9, 10, 12, 13, 16, 17, 20, 21, 22], others adopt a linear elastic one [4, 5, 6, 30, 42]. Tumours are therefore sometimes considered as an aggregate of soft balloons that roll on each other in a continuum limit (visco-elastic fluid) or take inspiration from biological soft tissues models (non-linear elasticity). These differences are somehow hidden in the equations when spherical symmetry and incompressibility are assumed, so that geometry dominates mechanics, but they become most evident when a real three-dimensional modelling is faced.
2. Some authors describe a tumour as a mixture of several biological components, while others restrict themselves to the one-component theory. In some cases, the flow field is provided

on the basis of an equation of Darcy type [3], as tumour cells actually form a special kind of granular material moving in the extracellular matrix (see, for instance, [18, 23, 34]).

3. The mathematical modelling of growth poses several questions about the stress–growth relationships and the possible inclusion of residual stress in the formulation; some authors neglect them [17], while others do not [1].

One aim of this paper is to critically collect in a unifying mathematical framework the many partial contributions sketched in the list above. We illustrate the mathematical properties of the equations that model a growing tumour as a mixture of three components (cell, matrix, liquid). Tumour remodelling evolves according to the classical mixture theory for biological tissues dating back to [28, 45] and specifically applied to tumour growth in many recent papers like those mentioned above. The emphasis is on the mechanical aspects, we neglect the influence of chemical factors, e.g., nutrients, chemoattractants, growth factors, metalloproteinases, that definitely play a major role in tumour evolution. In particular, in the present framework, cell reorganisation originates from tension only, cells are not active and their migratory self–ability is neglected.

The multiplicative decomposition of the deformation gradient into two (or more) factors is used for two purposes in this paper: modelling growth and plastic mechanical behaviour. The basic idea of this formalism dates back to the early work of Kroner and Lee in plasticity and has been reformulated by Rodriguez and co-workers in a biomechanical context as applied to growth [43]. In the specific field of tumour mechanics, Ambrosi and Mollica [2] apply this methodology to evaluate the residual stress formation in a growing multicellular spheroid described as a purely elastic one–component body. Although the qualitative behaviour of the solution is the expected one, the tension they find by numerical simulations is very large and this suggests that in their fully elastic model some mechanism of stress relaxation is neglected.

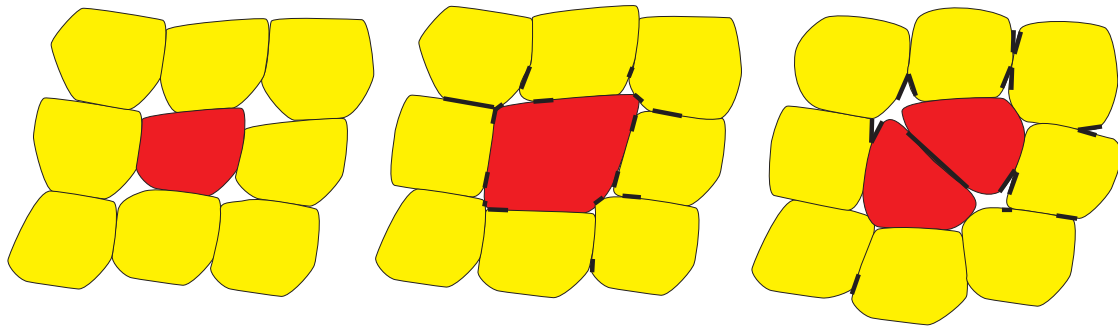
In the present paper stress relaxation at a macroscopic level is introduced on the basis of cellular arguments. It is known that cells adhere each other via cadherin junctions and to the extra-cellular matrix via integrin junctions. In standard experiments to test the adhesive strength of a cell, a microsphere adheres to the tip of an atomic force microscopy cantilever, the microsphere is posed in contact with the cell and then the cantilever is pulled away at a constant speed. Typical experimental plots of force vs. displacement are shown in Fig. 1; the characteristic strength of a bond has been measured, for instance, by Baumgardner et al. [8], Canetta et al. [14], Panorchan et al. [37], and Sun *et al.* [48].

Baumgardner et al. [8] properly functionalise a bead to achieve a strong attachment with the vascular endothelial cadherins secreted by transfected Chinese hamster ovary cells and allow a resting time on the cell surface of the order of one second. When the cantilever is pulled away at a constant speed (in the range  $0.2\text{--}4\ \mu\text{m}/\text{sec}$ ) the adhesion force deflects the cantilever. The plot of the bending force in time is characterised by several jumps, indicating the rupture of adhesive bonds, as shown in Fig. 1c. Actually, since a sphere binds to many receptors, multiple unbinding events occur at different times, as shown by the grey curve in Fig. 1c. The height of such jumps suggests that the adhesive strength of a single bond is in the range of 35–55 pN.

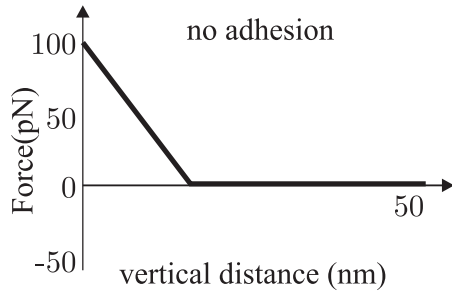
A similar experiment is reported by Sun et al. [48] without bead functionalization and allowing a longer resting time on the cell surface, ranging from 2 to 30 seconds. Chinese hamster ovary cells, endothelial cells and human brain tumour cells are used. Again, pulling away the cantilever at a constant speed in the range  $3\text{--}5\ \mu\text{m}/\text{sec}$  adhesive bonds break. All cell types indicate the maximum adhesive strength of a single bond to be slightly below 30 pN. Coating the bead with poly-L-lysine or collagen did not yield significant changes in the measurement.

Panorchan et al. [37] attach to the cantilever a cadherin-expressing cell, similar to the cell attached to the substratum. The time of contact is short, in order to have the formation of a very limited number of adhesion bonds. The rupture force is found to increase with the loading rate and it is much smaller when N-cadherin bonds are involved (up to 40 pN) rather than E-cadherin bonds (up to 73 pN for a loading rate of 1000 pN/s and 157 pN for a loading rate of 10000 pN/s).

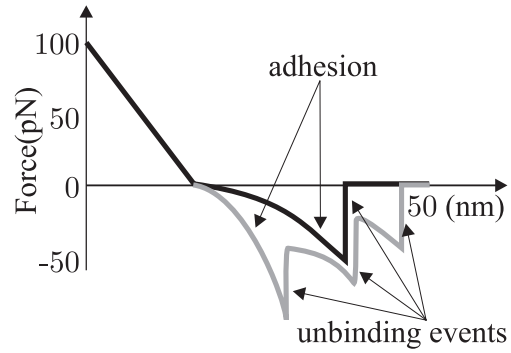
Interfering with the adhesion mechanism gives rise to big differences. Baumgardner et al. [8] add an antibody of the vascular endothelial cadherin external domain and the behaviour of the



(a)



(b)



(c)

Figure 1: (a) Sketch of plastic behaviour during tumour growth. Thicker lines indicate where there is a reorganisation of adhesion bonds, e.g., broken or newly formed. (b) and (c) refer to classical output from adhesive force measurement (redrawn from [8, 37, 48]). Adhesiveness acts as an elastic non-linear spring. However, when the force is too strong, then bonds break, giving rise to single or multiple unbinding events.

measured force is of the type shown in Fig. 1b, thus suggesting that there is no adhesion. A similar method is used in [37] to verify the specificity of cadherin-mediated interaction.

Sun et al. [48] use latrunculin A to disrupt the actin cytoskeleton in a concentration dependent way. In these cases the adhesion decreases down to 15 pN. A comparable result is obtained treating the cells with hyaluronidase. A similar ratio is obtained by Canetta et al. [14] who measure the adhesion force of intercellular adhesion molecules-1 (ICAM-1) linked or not linked to the actin cytoskeleton depending on the expression of a mutant form of ICAM-1 without its cytoplasmic domain.

The experimental cellular (molecular) behavior reported above can then be schematised as follows: if an ensemble of cells is subject to a sufficiently high tension, locally some bonds break and some others form. At a tissue level this argument suggests the introduction of a yield stress and the use of plastic deformations formalism of continuum mechanics. In particular, the mechanism of cell attachment–detachment can be relevant during growth under an external load, when duplicating cells displace their neighbours only if the needed energy to make such a work is available, as sketched in Fig. 1a.

The paper then develops as follows. In the first section a general multiphase framework is developed considering the tumour as made of cells, extracellular matrix and extracellular liquid. The multiplicative decomposition of the deformation gradient is introduced in the same section. Section 2 describes a constitutive model able to include the yield stress. Limit cases are worked out in Section 3 to understand the link between previously applied models and the one presented here. Finally, in Section 4 a one-dimensional problem is studied numerically, showing how tumour growth can be influenced by stress, how and where it can generate plastic reorganisation of the cells, how it can lead to capsule formation and compression of the surrounding tissue.

# 1 The Multiphase Model

## Kinematics

A tumour is made of many constituents, including tumour cells, extracellular matrix (ECM) and extracellular liquid. Nutrients and chemical factors diffuse in the liquid and are absorbed/produced by the cells; they play a relevant energetic role in growth but not in mass and force balance and are neglected in the present work. Cells live, move and duplicate in the extracellular matrix. In the present work, we assume that the ECM is neither degraded nor produced by the cells. As usual in multiphase theory, we associate every component with its own deformation gradient defined in every point of the mixture. In the following we indicate the fields corresponding to the tumour, liquid and extracellular matrix by the subscripts  $(t, l, m)$ , respectively.

In the deformation gradient of the tumour component  $\mathbf{F}_t$  we distinguish the contributions due to pure growth, plastic deformation and elastic deformation by a multiplicative decomposition. This splitting is suggested also by the observation that growth occurs on a time scale much longer (hours up to days) than deformation.

The deformation gradient  $\mathbf{F}_t$  is a mapping from a tangent space onto another tangent space, and it indicates how the body is deforming locally going from the initial (reference) configuration  $\mathcal{K}_0$  to the current configuration  $\mathcal{K}_t$ . An imaginary intermediate configuration can be introduced assuming that a point of the body can relieve its state of stress while relaxing the continuity, i.e. the integrity of the body. It then relaxes to a stress-free configuration. The atlas of these pointwise configurations forms what we define natural configuration with respect to  $\mathcal{K}_t$  and denote by  $\mathcal{K}_n$ . Referring to Figure 2, we identify this deformation without growth with the tensor  $\mathbf{F}_n$ , which then describes how the body is deforming locally while going from the natural configuration  $\mathcal{K}_n$  to  $\mathcal{K}_t$ .

The particle in the configuration  $\mathcal{K}_n$  has possibly undergone growth and plastic deformation. One can then again consider the map from  $\mathcal{K}_0$  to  $\mathcal{K}_n$  as composed of two parts: the first one related to growth/death processes (therefore to mass variations in the volume element), the second one due to internal reorganisation, which implies re-arranging of the adhesion links among the cells,

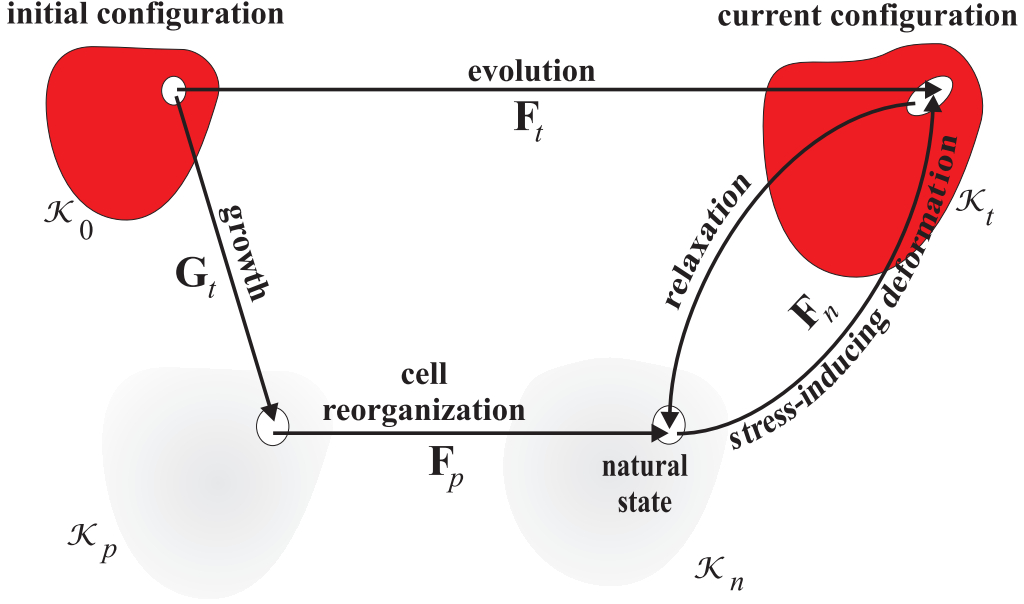


Figure 2: Multiple natural configuration.

without change of mass in the volume element. Denoting by  $\mathcal{K}_p$  the “grown configuration”, i.e., the intermediate configuration of the body between  $\mathcal{K}_0$  and  $\mathcal{K}_n$ , we will assume that for any given point the volume ratio in  $\mathcal{K}_p$  is the same as in the natural configuration  $\mathcal{K}_n$  and in the original reference configuration  $\mathcal{K}_0$ , i.e.,  $\phi_p = \phi_t(t=0) = \phi_n$ .

According to the three-steps process outlined above, the deformation gradient is split as

$$\mathbf{F}_t = \mathbf{F}_n \mathbf{F}_p \mathbf{G}_t. \quad (1.1)$$

Denoting by  $dV$ ,  $dV_p$ ,  $dV_n$ , and  $dv$  the volume elements in the initial, grown, natural and current configuration, respectively, the related masses are then  $dM = \rho\phi_n dV$ ,  $dm = \rho\phi_p dV_p = \rho\phi_n dV_n = \rho\phi_t dv$  where it can be noticed that mass is preserved between  $\mathcal{K}_p$  and  $\mathcal{K}_t$ , through  $\mathcal{K}_n$ . One then has that

$$\begin{aligned} J_t &= \det \mathbf{F}_t = \frac{dv}{dV} = \frac{\phi_n}{\phi_t} \frac{dm}{dM}, \\ J_g &= \det \mathbf{G}_t = \frac{dV_p}{dV} = \frac{\phi_n}{\phi_p} \frac{dm}{dM} = \frac{dm}{dM}, \\ J_p &= \det \mathbf{F}_p = \frac{dV_n}{dV_p} = \frac{\phi_p}{\phi_n} = 1, \\ J_n &= \det \mathbf{F}_n = \frac{dv}{dV_n} = \frac{\phi_n}{\phi_t}, \end{aligned} \quad (1.2)$$

and, of course,

$$J_t = J_g J_p J_n = J_g J_n. \quad (1.3)$$

Net growth corresponds to  $J_g > 1$  and net death to  $J_g < 1$ . Of course,  $J_g$  never vanishes, otherwise  $\mathbf{F}_t$  would be singular.

The mass balance equations for the constituents can be written as

$$\begin{aligned}\frac{\partial \phi_m}{\partial t} + \nabla \cdot (\phi_m \mathbf{v}_m) &= 0, \\ \frac{\partial \phi_t}{\partial t} + \nabla \cdot (\phi_t \mathbf{v}_t) &= \Gamma_t, \\ \frac{\partial \phi_\ell}{\partial t} + \nabla \cdot (\phi_\ell \mathbf{v}_\ell) &= -\Gamma_t.\end{aligned}\tag{1.4}$$

According to the terms on the r.h.s. the tumour exchanges mass with the extracellular liquid only at the rate  $\Gamma_t$ .

In order to find the relation between  $\Gamma_t$  and  $J_g$  we differentiate  $J_t = J_g J_n$  to get

$$\frac{1}{J_t} \frac{dJ_t}{dt} = \frac{1}{J_g} \frac{dJ_g}{dt} + \frac{1}{J_n} \frac{dJ_n}{dt},\tag{1.5}$$

where the time derivative is a convective derivative computed using the velocity of the transported component.

On the other hand differentiating the last equation in (1.2) one has that

$$\frac{d}{dt} \log(\phi_t J_n) = 0.\tag{1.6}$$

Hence, (1.5) rewrites

$$\frac{1}{J_g} \frac{dJ_g}{dt} = \frac{1}{\phi_t} \left( \frac{d\phi_t}{dt} + \frac{\phi_t}{J_t} \frac{dJ_t}{dt} \right),\tag{1.7}$$

so that using Equations (1.7) and (1.4) one can finally write

$$\frac{\dot{J}_g}{J_g} = \frac{1}{\phi_t} \left( \Gamma_t - \phi_t \nabla \cdot \mathbf{v}_t + \frac{\phi_t}{J_t} \dot{J}_t \right) = \frac{\Gamma_t}{\phi_t} + \frac{1}{J_t} \left( \dot{J}_t - J_t \nabla \cdot \mathbf{v}_t \right) = \frac{\Gamma_t}{\phi_t}.\tag{1.8}$$

where the upper dot denotes time differentiation following the tumour cells.

In the following we will assume spherical growth:  $\mathbf{G}_t = g\mathbf{I}$ . In this case  $J_g = g^3$  and (1.8) rewrites as

$$\dot{g} = \frac{\Gamma_t}{\phi_t} \frac{g}{3}.\tag{1.9}$$

Given  $\Gamma_t$ , the equation above describes how  $\mathbf{G}_t$  evolves as a function of  $\phi_t$  and all the other variables  $\Gamma_t$  depends upon, and therefore how  $\mathcal{K}_p$  evolves.

## Dynamics

The momentum equation for the constituents can be written neglecting inertia and assuming, as usual when dealing with slow flow in porous materials, that the interaction force between constituents is proportional to the relative velocity between the constituents themselves [3]. One then has

$$\begin{aligned}-\nabla \cdot \mathbf{T}_m + \phi_m \nabla P &= -\mathbf{M}_{tm}(\mathbf{v}_m - \mathbf{v}_t), \\ \phi_t \nabla P - \nabla \cdot \mathbf{T}_t &= -\mathbf{M}_{\ell t}(\mathbf{v}_t - \mathbf{v}_\ell) - \mathbf{M}_{tm}(\mathbf{v}_t - \mathbf{v}_m), \\ \phi_\ell \nabla P &= -\mathbf{M}_{\ell t}(\mathbf{v}_\ell - \mathbf{v}_t).\end{aligned}\tag{1.10}$$

Here we also assume that the interaction force between liquid and ECM is negligible compared to the interaction force exerted by the cells on the ECM or the drag of the cells by the liquid. More general constitutive models for cell-ECM interactions are studied in [41] and focus on adhesion mechanisms between cells and ECM.

Introducing the permeability tensor  $\mathbf{K} = \phi_\ell^2 \mathbf{M}_{\ell t}^{-1}$  and  $\mathbf{K}_m = \phi_m^2 \mathbf{M}_{mt}^{-1}$  into Equation (1.10) and substituting the last equation with the sum of the partial force balances, so to get the momentum equation of the mixture, one has

$$\begin{aligned} \frac{\mathbf{K}_m}{\phi_m^2} (-\phi_m \nabla P + \nabla \cdot \mathbf{T}_m) &= \mathbf{v}_m - \mathbf{v}_t \\ -\frac{\mathbf{K}}{\phi_\ell} \nabla P &= \mathbf{v}_\ell - \mathbf{v}_t \\ -\nabla P + \nabla \cdot (\mathbf{T}_m + \mathbf{T}_t) &= 0. \end{aligned} \tag{1.11}$$

The stress tensors in the equations above account for partial stress, i.e. the stress of each component in the mixture, which must depend on the corresponding volume fraction at least linearly, as remarked for instance in Truesdell [25].

## 2 Stress Constitutive Model

This section is devoted to stating the constitutive assumptions for the components of the mixture. We assume that the ECM behaves as a compressible elastic body, satisfying

$$\mathbf{T}_m = \phi_m \hat{\mathbf{T}}_m(\mathbf{B}_m), \tag{2.1}$$

where  $\mathbf{B}_m = \mathbf{F}_m \mathbf{F}_m^T$ .

On the other hand, inclusion of visco-plastic effects in the mechanics of cell aggregates goes along the following intuitive description:

1. when and where the cell populations is subject to a moderate amount of stress, then the body behaves elastically;
2. when and where the stress overcomes a threshold yield stress then the body undergoes visco-plastic deformations.

Defining

$$\mathbf{D}_p = \text{sym}(\dot{\mathbf{F}}_p \mathbf{F}_p^{-1}), \tag{2.2}$$

from standard tensor calculus one has that

$$\dot{J}_p = J_p \text{tr} \mathbf{D}_p, \tag{2.3}$$

and therefore because of (1.2)<sub>3</sub>

$$\text{tr} \mathbf{D}_p = 0. \tag{2.4}$$

The definition of yield stress can be argued on the basis of the mechanism sketched in Fig. 1. Given the resistance of a single bond, the threshold of the onset of plastic deformations is proportional to the area of the cell membranes in contact, that depends on the number of cells per unit volume. In absence of additional experimental support, we assume a proportionality rule between yield stress and tumour cells volume fraction though, in reality, the relation might be more complex. In fact a very small, volume ratio can correspond to much dispersed single cells or very clusterized ensembles. In the former case, the yield stress is expected to be very low. In the second case, borrowing ideas from the dynamics of colloidal particles and flocculated suspensions, the yield stress should increase with the second or the third power of the volume ratio [11, 47].

On this basis, the following elastic-type constitutive equation can be suggested in the elastic regime

$$\mathbf{T}_t = \phi_t \hat{\mathbf{T}}_t(\mathbf{B}_n), \quad \text{if } f(\mathbf{T}_t) \leq \phi_t \tau, \tag{2.5}$$

where  $\mathbf{B}_n = \mathbf{F}_n \mathbf{F}_n^T$  and  $\tau$  is a measure of the yield stress.

The function  $f(\mathbf{T}_t)$  is a frame invariant measure of the stress, vanishing for  $\mathbf{T}_t = 0$ , homogeneous of degree one, i.e.

$$f(\alpha \mathbf{T}_t) = |\alpha| f(\mathbf{T}_t), \tag{2.6}$$

to be specified in the following.

Following [7, 46], above the yield stress the tension in excess originates from cell unbinding at the microscopic scale and then cell rearrangement at the macroscopic scale. Such a pictorial description is put into formal terms by the following constitutive equation

$$\left[1 - \frac{\phi_t \tau}{f(\mathbf{T}_t - \frac{1}{3}(\text{tr}\mathbf{T}_t)\mathbf{I})}\right] \left(\mathbf{T}_t - \frac{1}{3}(\text{tr}\mathbf{T}_t)\mathbf{I}\right) = 2\eta_p \phi_t \tilde{\mathbf{D}}_p, \quad \text{if } f\left(\mathbf{T}_t - \frac{1}{3}(\text{tr}\mathbf{T}_t)\mathbf{I}\right) > \phi_t \tau, \quad (2.7)$$

where  $\tilde{\mathbf{D}}_p = \mathbf{F}_n \mathbf{D}_p \mathbf{F}_n^{-1}$ . Notice that the left hand side of equation (2.7) is traceless and therefore the incompressibility constraint (2.4) always applies while the factor in square brackets on the left hand side is always positive.

We observe that using the more general form

$$\left[1 - \frac{\phi_t \tau}{f(\mathbf{T}_t - \alpha\mathbf{I})}\right] (\mathbf{T}_t - \alpha\mathbf{I}) = -\beta\mathbf{I} + 2\eta_p \phi_t \tilde{\mathbf{D}}_p, \quad \text{if } f(\mathbf{T}_t - \alpha\mathbf{I}) > \phi_t \tau, \quad (2.8)$$

with generic  $\alpha$  and  $\beta$  leads again to (2.7). In fact, applying the trace operator and recalling Eq. (2.4), one has that  $\alpha = \frac{1}{3}(\text{tr}\mathbf{T}_t)$  and  $\beta = 0$ .

It is instructive to look closely at what happens at criticality, i.e. when

$$f\left(\mathbf{T}_t - \frac{1}{3}(\text{tr}\mathbf{T}_t)\mathbf{I}\right) = \phi_t \tau. \quad (2.9)$$

In this case, Eq. (2.7) implies that  $\mathbf{D}_p = 0$  (and therefore  $\dot{\mathbf{F}}_p = 0$ ) which means that no contribution to the evolution of the natural configuration is due to plastic deformations, while the system stays on (or inside) the yield surface. A contribution is instead generated when the system crosses the yield surface.

The relationship (2.7) can be rewritten in a more usual form applying the function  $f$  to both sides of (2.7), giving the relation

$$f\left(\left[1 - \frac{\phi_t \tau}{f(\mathbf{T}_t - \frac{1}{3}(\text{tr}\mathbf{T}_t)\mathbf{I})}\right] \left(\mathbf{T}_t - \frac{1}{3}(\text{tr}\mathbf{T}_t)\mathbf{I}\right)\right) = f(2\eta_p \phi_t \tilde{\mathbf{D}}_p), \quad (2.10)$$

or, thanks to the homogeneity of  $f$  expressed in (2.6),

$$2\eta_p \phi_t f(\tilde{\mathbf{D}}_p) = \left[1 - \frac{\phi_t \tau}{f(\mathbf{T}_t - \frac{1}{3}(\text{tr}\mathbf{T}_t)\mathbf{I})}\right] f\left(\mathbf{T}_t - \frac{1}{3}(\text{tr}\mathbf{T}_t)\mathbf{I}\right) = f\left(\mathbf{T}_t - \frac{1}{3}(\text{tr}\mathbf{T}_t)\mathbf{I}\right) - \phi_t \tau. \quad (2.11)$$

This relation can be substituted back in (2.7) to give

$$\left[1 - \frac{\phi_t \tau}{\phi_t \tau + 2\eta_p \phi_t f(\mathbf{D}_p)}\right] \left(\mathbf{T}_t - \frac{1}{3}(\text{tr}\mathbf{T}_t)\mathbf{I}\right) = 2\eta_p \phi_t \tilde{\mathbf{D}}_p, \quad \text{if } f\left(\mathbf{T}_t - \frac{1}{3}(\text{tr}\mathbf{T}_t)\mathbf{I}\right) > \phi_t \tau, \quad (2.12)$$

or

$$\mathbf{T}_t = \frac{1}{3}(\text{tr}\mathbf{T}_t)\mathbf{I} + \left[2\eta_p + \frac{\tau}{f(\mathbf{D}_p)}\right] \phi_t \tilde{\mathbf{D}}_p, \quad \text{if } f\left(\mathbf{T}_t - \frac{1}{3}(\text{tr}\mathbf{T}_t)\mathbf{I}\right) > \phi_t \tau, \quad (2.13)$$

which more closely resembles the usual form of constitutive equation of Bingham fluids used in the literature. However, in the following sections we refer to the form (2.7) because it directly provides the evolution of  $\mathbf{F}_p$ .

There are several possible choices of the function  $f$ . The three-dimensional generalisation of Bingham constitutive law proposed by Hohenemser and Prager [27] reads

$$f(\mathbf{P}) \equiv f_1(\mathbf{P}') = \sqrt{\frac{\mathbf{P}' : \mathbf{P}'}{2}}, \quad (2.14)$$

where  $\mathbf{P}' = \mathbf{P} - \frac{\text{tr}\mathbf{P}}{3}\mathbf{I}$ . Basov and Shelukhin [7] instead suggest to base the measure on

$$\mathbf{p}(\mathbf{n}) = \mathbf{P}\mathbf{n} - (\mathbf{n} \cdot \mathbf{P}\mathbf{n})\mathbf{n}, \quad (2.15)$$

that represents the tangential stress vector relative to the surface identified by the normal  $\mathbf{n}$ . Therefore the quantity

$$f(\mathbf{P}) \equiv f_2(\mathbf{P}) = \max_{|\mathbf{n}|=1} |\mathbf{p}(\mathbf{n})|, \quad (2.16)$$

is the maximum shear stress magnitude occurring in the plane identified by the eigenvector corresponding to the maximum of  $|\mathbf{p}(\mathbf{n})|$ . It can be proved (see, for instance, [35]) that  $f_2$  is given by half of the difference between the maximum and the minimum eigenvalue of  $\mathbf{P}$ .

Besov and Shelukin [7] suggest the following form:

$$f(\mathbf{P}) = f_3(\mathbf{P}) = \sqrt{f_2^2(\mathbf{P}) + (\text{tr}\mathbf{P})^2}.$$

However, in our case the argument of  $f$  is traceless and therefore  $f_2 = f_3$ .

In conclusion, assuming that the tumour component obeys to a neo-Hookean non-linear elastic law, the following constitutive equation can be suggested

$$\mathbf{T}_t = \phi_t(-\Sigma_t\mathbf{I} + \mu_t\mathbf{B}_n) = \phi_t\left(-\Sigma_t\mathbf{I} + \frac{\mu_t}{g^2}\mathbf{F}_t\mathbf{C}_p^{-1}\mathbf{F}_t^T\right), \quad (2.17)$$

where  $\Sigma_t = \Sigma_t(\phi_t/\phi_n)$ , with  $\Sigma_t(1) = \mu_t$ , and  $\mathbf{C}_p = \mathbf{F}_p^T\mathbf{F}_p$ , and  $\mathbf{F}_p$  evolves according to

$$\dot{\mathbf{F}}_p = \begin{cases} \mathbf{0}, & \text{if } f(\mathbf{B}_n - \frac{1}{3}(\text{tr}\mathbf{B}_n)\mathbf{I}) \leq \frac{\tau}{\mu_t}; \\ \frac{\mu_t}{2\eta_p} \left[ 1 - \frac{\tau}{\mu_t f(\mathbf{B}_n - \frac{1}{3}(\text{tr}\mathbf{B}_n)\mathbf{I})} \right] \mathbf{F}_n^{-1} \left( \mathbf{B}_n - \frac{1}{3}(\text{tr}\mathbf{B}_n)\mathbf{I} \right) \mathbf{F}, & \text{if } f(\mathbf{B}_n - \frac{1}{3}(\text{tr}\mathbf{B}_n)\mathbf{I}) > \frac{\tau}{\mu_t}. \end{cases} \quad (2.18)$$

or, in a more compact form,

$$\dot{\mathbf{F}}_p = \frac{\mu_t}{2\eta_p} \left[ 1 - \frac{\tau}{\mu_t f(\mathbf{B}_n - \frac{1}{3}(\text{tr}\mathbf{B}_n)\mathbf{I})} \right]_+ \mathbf{F}_n^{-1} \left( \mathbf{B}_n - \frac{1}{3}(\text{tr}\mathbf{B}_n)\mathbf{I} \right) \mathbf{F}, \quad (2.19)$$

where  $[\cdot]_+$  stands for the positive part of the argument.

It is of course possible to generalise the constitutive model above to include possible shear-thinning effects by allowing a dependence of  $\eta_p$  from  $\mathbf{D}_p$ , e.g.,

$$\eta_p = m|\mathbb{I}_{D_p}|^{(n-1)/2} \quad (2.20)$$

where the coefficient  $n$  is related to the slope of the shear stress behaviour versus the shear rate. In this way one obtains a constitutive equation similar to Herschel–Buckley model.

In order to explain phenomenologically Eq. (2.19), consider the case of absence of growth. If the body undergoes a deformation corresponding to a stress below the yield stress, then  $\mathbf{F}_p$  does not change, i.e., the intermediate configuration does not evolve and all the energy is elastically stored. If the measure of tension  $f$  takes a value larger than the yield stress, then the reference configuration changes to release the stress in excess, until the yield surface defined by  $f$  is reached again. The ratio  $\eta_p/\mu_t$  gives an indication of the characteristic time needed to reach the yield surface.

### 3 Limit Cases

In this section we examine how our model compares with previously proposed ones. In fact, some attempts were done in the literature to describe growing tumours alternatively as elastic solids

[4, 5, 6, 30] or fluids [3, 9, 10, 12, 13, 16, 17, 20, 21, 22], including stress relaxation while avoiding the split of the deformation gradient into growth and deformation. Usual assumptions in the former case are incompressibility of the cell component and a linear elastic behaviour. Plastic or visco-plastic deformations are not taken into account.

More specifically, Jones and co-workers [30] and Araujo and McElwain [4, 5, 6] propose

$$\mathbf{T}'_t = \frac{2}{3}E \left( \mathbf{E}_t - \frac{1}{3}(\text{tr}\mathbf{E}_t)\mathbf{I} \right), \quad (3.21)$$

where  $\mathbf{T}'_t = \mathbf{T}_t - \frac{1}{3}(\text{tr}\mathbf{T}_t)\mathbf{I}$  and  $\mathbf{E}_t$  is the infinitesimal strain tensor. The same Authors propose to rewrite the constitutive equation in terms of the rate of stress as

$$\dot{\mathbf{T}}'_t + \mathbf{W}_t \mathbf{T}'_t - \mathbf{T}'_t \mathbf{W}_t = \frac{2}{3}E \left( \mathbf{D}_t - \frac{1}{3}(\nabla \cdot \mathbf{v}_t)\mathbf{I} \right) \quad (3.22)$$

where  $\mathbf{W}_t = (\nabla \mathbf{v}_t - \nabla \mathbf{v}_t^T)/2$  is the vorticity tensor. The particular time derivative appearing at the left hand side of equation (3.22) yields a frame indifferent relationship, provided that  $\mathbf{T}_t$  is frame invariant. Unfortunately, this is no case for  $\mathbf{T}_t$  in (3.21) and for  $\mathbf{E}_t$  and therefore its use is inappropriate in the linear theory (see, for instance, [35], page 403).

In order to compare Equations (3.21) and (3.22) with the model proposed in the present paper, a linear version has to be obtained in the small strain limit.

The small deformation assumption applies depending on the value of the yield stress: it has to be small enough so that the condition  $|\mathbf{B}_n \cdot \mathbf{I} - 3| \ll 1$  is always satisfied during the motion. Note that for tensions larger than 0.1 kPA, cell adhesion bonds break up [8], thus giving an indication of the order of magnitude of the yield stress. For small elastic strain one can use linear elasticity below the yield surface. For larger stress, the natural configuration evolves. If the relaxation of stresses is much faster than growth, as it should be, then the deformation with respect to the natural configuration due to growth are kept small during the evolution.

To compare our result with previous works we impose the incompressibility constraint to tumour matter ( $J_n = 1$ ), the spherical part of the stress tensor is replaced by a Lagrangean multiplier  $P_t$ , so that the elastic constitutive equation rewrites

$$\mathbf{T}'_t = \mu_t \phi_n \left( \mathbf{B}_n - \frac{1}{3}(\text{tr}\mathbf{B}_n)\mathbf{I} \right), \quad (3.23)$$

where  $\mathbf{T}_t = -P_t \mathbf{I} + \mathbf{T}'_t$ . Deriving (3.23) in time, one has

$$\dot{\mathbf{T}}'_t = \mu_t \phi_n \left( \dot{\mathbf{B}}_n - \frac{1}{3}(\text{tr}\dot{\mathbf{B}}_n)\mathbf{I} \right), \quad (3.24)$$

where

$$\dot{\mathbf{B}}_n = \mathbf{L}_n \mathbf{B}_n + \mathbf{B}_n \mathbf{L}_n^T, \quad (3.25)$$

with

$$\mathbf{L}_n = \dot{\mathbf{F}}_n \mathbf{F}_n^{-1}. \quad (3.26)$$

On the other hand, deriving  $\mathbf{F}_t = g \mathbf{F}_n \mathbf{F}_p$  in time, one has

$$\begin{aligned} \dot{\mathbf{F}}_t &= \dot{g} \mathbf{F}_n \mathbf{F}_p + g \dot{\mathbf{F}}_n \mathbf{F}_p + g \mathbf{F}_n \dot{\mathbf{F}}_p = \dot{g} g^{-1} \mathbf{F}_t + g \mathbf{L}_n \mathbf{F}_n \mathbf{F}_p + g \mathbf{F}_n \mathbf{D}_p \mathbf{F}_p \\ &= (\dot{g} g^{-1} \mathbf{I} + \mathbf{L}_n + \mathbf{F}_n \mathbf{D}_p \mathbf{F}_n^{-1}) \mathbf{F}_t. \end{aligned} \quad (3.27)$$

Hence, defining as usual,  $\mathbf{L}_t = \dot{\mathbf{F}}_t \mathbf{F}_t^{-1}$  one can write

$$\mathbf{L}_n = \mathbf{L}_t - \dot{g} g^{-1} \mathbf{I} - \mathbf{F}_n \mathbf{D}_p \mathbf{F}_n^{-1}, \quad (3.28)$$

which can be substituted back in (3.25) to give

$$\dot{\mathbf{B}}_n = \mathbf{L}_t \mathbf{B}_n + \mathbf{B}_n \mathbf{L}_t^T - 2\dot{g} g^{-1} \mathbf{B}_n - 2\mathbf{F}_n \mathbf{D}_p \mathbf{F}_n^T. \quad (3.29)$$

In the limit of small deformations, (3.29) reduces to leading order to

$$\dot{\mathbf{B}}_n \approx 2(\mathbf{D}_t - \dot{g}g^{-1}\mathbf{I} - \mathbf{D}_p). \quad (3.30)$$

Recalling that  $\text{tr}\mathbf{D}_p = 0$ , one then has that

$$\dot{\mathbf{B}}_n - \frac{1}{3}(\text{tr}\dot{\mathbf{B}}_n)\mathbf{I} \approx 2\left(\mathbf{D}_t - \mathbf{D}_p - \frac{1}{3}(\text{tr}\mathbf{D}_t)\mathbf{I}\right), \quad (3.31)$$

and therefore from (3.24)

$$\dot{\mathbf{T}}'_t = 2\mu_t\phi_n\left(\mathbf{D}_t - \mathbf{D}_p - \frac{1}{3}(\nabla \cdot \mathbf{v}_t)\mathbf{I}\right), \quad (3.32)$$

or, recalling (2.7),

$$\dot{\mathbf{T}}'_t + \frac{\mu_t}{\eta_p}\left[1 - \frac{\phi_n\tau}{f(\mathbf{T}'_t)}\right]_+ \mathbf{T}'_t = 2\mu_t\phi_n\left(\mathbf{D}_t - \frac{1}{3}(\nabla \cdot \mathbf{v}_t)\mathbf{I}\right). \quad (3.33)$$

where due to the incompressibility condition  $\nabla \cdot \mathbf{v}_t = \Gamma_t/\phi_n$ . Therefore, one has

$$\dot{\mathbf{T}}'_t + \frac{\mu_t}{\eta_p}\left[1 - \frac{\phi_n\tau}{f(\mathbf{T}'_t)}\right]_+ \mathbf{T}'_t = 2\mu_t\left(\phi_n\mathbf{D}_t - \frac{\Gamma_t}{3}\mathbf{I}\right). \quad (3.34)$$

In absence of plastic deformation, i.e., for  $f(\mathbf{T}'_t) < \phi_n\tau$ , (3.34) reduces to the constitutive model proposed in [4, 5, 6, 30] (with  $E = 3\mu_t\phi_n$  and dropping the convective derivatives).

On the other hand, we observe that in (3.34), the term containing the yield stress plays the role of a stress relaxation term that switches on just when the stress is above the yield value.

As in classical viscoelasticity [24, 29], the ratio  $\eta_p/\mu_t$  identifies the characteristic time needed to relax the stress to the yield value (not the null one, as in Maxwell fluids) and will be called here *plastic rearrangement time*. The limit  $\eta_p \gg \mu_t$  leads again to [4, 5, 6, 30]. However, in this case the procedure is incompatible with the small deformation assumption because the stress relaxes very slowly and so large stresses and deformation can build up.

On the other hand, rewriting (3.34) as

$$\frac{\eta_p}{\mu_t}\dot{\mathbf{T}}'_t + \left[1 - \frac{\phi_n\tau}{f(\mathbf{T}'_t)}\right]_+ \mathbf{T}'_t = 2\eta_p\left(\phi_n\mathbf{D}_t - \frac{\Gamma_t}{3}\mathbf{I}\right), \quad (3.35)$$

it is easy to realise that the limit  $\eta_p \ll \mu_t$  with  $\tau$  tending to zero leads to the viscous limit with viscosity  $\eta_p$  is used as a constitutive model for a constrained mixture [20, 21, 22]. Following the same argument proposed in [40, 39] one can state that in transient phenomena for times much larger than *plastic rearrangement time* the natural configuration has evolved relaxing the stress, leaving the material in a state of stress living on the yield surface.

## 4 One-Dimensional Problems

The equations of motion simplify considerably in the case of one-dimensional motion. The most important simplification is that the deformation tensor can be described by a scalar quantity that relates Eulerian and Lagrangean co-ordinates through the volume ratio. The second simplification is that in one dimension a divergence-free velocity field is constant.

In fact, in one-dimensional problems Equations (1.4) and (1.11) lead to the following system

of equations in the  $(z, t)$  independent variables

$$\left\{ \begin{array}{l} \frac{\partial \phi_m}{\partial t} + \frac{\partial}{\partial z}(\phi_m v_m) = 0, \\ \frac{\partial \phi_t}{\partial t} + \frac{\partial}{\partial z}(\phi_t v_t) = \Gamma_t, \\ \frac{\partial}{\partial z}(\phi_m v_m + \phi_t v_t + \phi_\ell v_\ell) = 0, \\ v_\ell - v_t = -\frac{K}{\phi_\ell} \frac{\partial P}{\partial z}, \\ v_m - v_t = \frac{K_m}{\phi_m^2} \left( -\phi_m \frac{\partial P}{\partial z} + \frac{\partial T_m}{\partial z} \right), \\ -\frac{\partial P}{\partial z} + \frac{\partial}{\partial z}(T_m + T_t) = 0, \end{array} \right. \quad (4.1)$$

where to simplify the notation we denoted by  $T_m$  and  $T_t$  the stresses  $T_{m,zz}$  and  $T_{t,zz}$ , respectively.

Equation (4.1)<sub>3</sub> implies that  $\phi_m v_m + \phi_t v_t + \phi_\ell v_\ell = 0$  and the system (4.1) simplifies to

$$\begin{aligned} v_m &= \left( K + \frac{(1 - \phi_m)^2}{\phi_m^2} K_m \right) \frac{\partial T_m}{\partial z} + \left( K - \frac{1 - \phi_m}{\phi_m} K_m \right) \frac{\partial T_t}{\partial z}, \\ v_\ell &= \left( -\frac{\phi_t + \phi_m}{1 - \phi_t - \phi_m} K - \frac{1 - \phi_m}{\phi_m} K_m \right) \frac{\partial T_m}{\partial z} + \left( -\frac{\phi_t + \phi_m}{1 - \phi_t - \phi_m} K + K_m \right) \frac{\partial T_t}{\partial z}, \\ v_t &= \left( K - \frac{1 - \phi_m}{\phi_m} K_m \right) \frac{\partial T_m}{\partial z} + (K + K_m) \frac{\partial T_t}{\partial z}. \end{aligned} \quad (4.2)$$

In particular, combining the mass balance equations with the form assumed by the velocity fields in (4.2) one can write

$$\left\{ \begin{array}{l} \frac{\partial \phi_m}{\partial t} + \frac{\partial}{\partial z} \left[ \left( \phi_m K + \frac{(1 - \phi_m)^2}{\phi_m} K_m \right) \frac{\partial T_m}{\partial z} + \phi_m (K + K_m) \frac{\partial T_t}{\partial z} \right] = 0, \\ \frac{\partial \phi_t}{\partial t} + \frac{\partial}{\partial z} \left[ \phi_t \left( K + \frac{1 - \phi_m}{\phi_m} K_m \right) \frac{\partial T_m}{\partial z} + (K + K_m) \frac{\partial T_t}{\partial z} \right] = \Gamma_t. \end{array} \right. \quad (4.3)$$

Notice that if the ECM is very soft, i.e.  $T_m \ll T_t$ , then

$$\begin{aligned} v_t &\approx (K + K_m) \frac{\partial T_t}{\partial z}, \\ v_m &\approx v_t - \frac{K_m}{\phi_m} \frac{\partial T_t}{\partial z}. \end{aligned}$$

On the other extreme, if the ECM is rigid ( $v_m = 0$ ) then

$$v_t = \frac{K K_m}{K \phi_m^2 + K_m (1 - \phi_m)^2} \frac{\partial T_t}{\partial z},$$

which implies that there is no motion if either  $K$  or  $K_m$  goes to zero. In the former case, in fact the space is occupied by fibres. In the latter, adhesion with the fibres is quite strong. If  $\phi_m \rightarrow 0$ , then  $v_t = K \partial T_t / \partial z$ , which is the type of relation used for instance in [16].

## 4.1 Homogeneous Growth of a Tumour in a Cylindrical Duct

To be more specific consider the case in which the tumour homogeneously grows inside a rigid cylinder. This situation resembles, for instance, the growth of a ductal carcinoma. Since the

cylinder walls are supposed to be rigid, we assume deformations and velocities of all constituents to be along the duct axis  $z$ . Focusing on the extracellular matrix one then has

$$\mathbf{F}_m = \text{Diag}\{1, 1, J_m\}, \quad \mathbf{B}_m = \text{Diag}\{1, 1, J_m^2\}, \quad \text{with} \quad J_m = \frac{\bar{\phi}_m}{\phi_m}, \quad (4.4)$$

where  $\text{Diag}\{\cdot\}$  stands for a diagonal matrix and  $\bar{\phi}_m$  is the ECM volume ratio in the reference configuration. Similarly for the tumour

$$\mathbf{F}_t = \text{Diag}\{1, 1, \Lambda_t\}, \quad \mathbf{F}_n = \text{Diag}\{\lambda_n, \lambda_n, \Lambda_n\}, \quad \mathbf{F}_p = \text{Diag}\{\lambda_p, \lambda_p, \Lambda_p\}, \quad (4.5)$$

and

$$\mathbf{B}_n = \text{Diag}\{\lambda_n^2, \lambda_n^2, \Lambda_n^2\}, \quad \mathbf{D}_p = \text{Diag}\{\dot{\lambda}_p \lambda_p^{-1}, \dot{\lambda}_p \lambda_p^{-1}, \dot{\Lambda}_p \Lambda_p^{-1}\}. \quad (4.6)$$

Equations (1.1), (1.2c), and (1.2d) imply that

$$\begin{cases} F_{t,rr} = 1 = \lambda_n \lambda_p g, \\ F_{t,zz} = \Lambda_t = \Lambda_n \Lambda_p g, \\ \det(\mathbf{F}_p) = 1 = \lambda_p^2 \Lambda_p, \\ \det(\mathbf{F}_n) = \frac{\phi_n}{\phi_t} = \lambda_n^2 \Lambda_n, \end{cases} \quad (4.7)$$

that can be solved to give

$$\Lambda_t = \frac{\phi_n}{\phi_t} g^3, \quad \lambda_n = \frac{\sqrt{\Lambda_p}}{g}, \quad \Lambda_n = \frac{\phi_n g^2}{\phi_t \Lambda_p}, \quad \lambda_p = \frac{1}{\sqrt{\Lambda_p}}. \quad (4.8)$$

We explicitly remark that given  $\Lambda_p$  and  $g$ ,  $B_{zz}$  is given by

$$B_{zz} = \frac{\phi_n^2}{\phi_t^2} \frac{g^4}{\Lambda_p^2}.$$

It is instructive to examine the case  $B_{zz} = 1$ , corresponding to no elastic deformations along the duct axis. For instance, if  $\phi_t = \phi_n$  and the body is growing,  $\Lambda_p$  must be such that  $\Lambda_p = g^2 > 1$  to achieve that, i.e., the body has to plastically rearrange and adapt in response to growth.

Now Bingham's constitutive equation for the evolution of  $\mathbf{F}_p$  gives

$$\dot{\lambda}_p = \dot{\Lambda}_p = 0, \quad \text{if} \quad f\left(\mathbf{B}_n - \frac{1}{3}(\text{tr}\mathbf{B}_n)\mathbf{I}\right) \leq \frac{\tau}{\mu_t}, \quad (4.9)$$

where if we choose  $f = f_2$  (see (2.16) applied to (2.17)), the yield condition reads

$$\frac{|\Lambda_n^2 - \lambda_n^2|}{2} \leq \tilde{\tau}, \quad (4.10)$$

where  $\tilde{\tau} = \tau/\mu_t$  and

$$\begin{aligned} \dot{\lambda}_p &= \lambda_p \frac{\mu_t}{2\eta_p} \left[ 1 - \frac{\tau}{\mu_t f(\mathbf{B}_n - \frac{1}{3}(\text{tr}\mathbf{B}_n)\mathbf{I})} \right] \left( \lambda_n^2 - \frac{1}{3}(2\lambda_n^2 + \Lambda_n^2) \right) \\ &= \lambda_p \frac{\mu_t}{2\eta_p} \left[ 1 - \frac{\tilde{\tau}}{f(\mathbf{B}_n - \frac{1}{3}(\text{tr}\mathbf{B}_n)\mathbf{I})} \right] \frac{\lambda_n^2 - \Lambda_n^2}{3}, \end{aligned} \quad (4.11)$$

$$\begin{aligned} \dot{\Lambda}_p &= \Lambda_p \frac{\mu_t}{2\eta_p} \left[ 1 - \frac{\tau}{\mu_t f(\mathbf{B}_n - \frac{1}{3}(\text{tr}\mathbf{B}_n)\mathbf{I})} \right] \left( \Lambda_n^2 - \frac{1}{3}(2\lambda_n^2 + \Lambda_n^2) \right) \\ &= \Lambda_p \frac{\mu_t}{\eta_p} \left[ 1 - \frac{\tilde{\tau}}{f(\mathbf{B}_n - \frac{1}{3}(\text{tr}\mathbf{B}_n)\mathbf{I})} \right] \frac{\Lambda_n^2 - \lambda_n^2}{3}, \end{aligned} \quad (4.12)$$

otherwise.

It can be easily checked that Eq.(2.4) holds and

$$\begin{aligned} \dot{J}_p &= 2\lambda_p \dot{\lambda}_p \Lambda_p + \lambda_p^2 \dot{\Lambda}_p \\ &= 2\lambda_p^2 \Lambda_p \frac{\mu_t}{2\eta_p} \left[ 1 - \frac{\tilde{\tau}}{f(\mathbf{B}_n)} \right] \frac{\lambda_n^2 - \Lambda_n^2}{3} + \lambda_p^2 \Lambda_p \frac{\mu_t}{\eta_p} \left[ 1 - \frac{\tilde{\tau}}{f(\mathbf{B}_n)} \right] \frac{\Lambda_n^2 - \lambda_n^2}{3} = 0. \end{aligned} \quad (4.13)$$

Using Eq.(4.8), (4.9)–(4.12) can be summarized in

$$\dot{\Lambda}_p = \frac{\mu_t}{3\eta_p} \left[ 1 - \frac{\tilde{\tau}}{f(\mathbf{B}_n)} \right]_+ \left( \frac{\phi_n^2}{\phi_t^2} \frac{g^4}{\Lambda_p} - \frac{\Lambda_p^2}{g^2} \right), \quad (4.14)$$

where

$$f(\mathbf{B}_n) = \frac{1}{2} \left( \frac{\phi_n^2}{\phi_t^2} \frac{g^4}{\Lambda_p} - \frac{\Lambda_p}{g^2} \right). \quad (4.15)$$

In particular, the yield condition (4.10) is given by

$$\frac{1}{2} \left| \frac{\phi_n^2}{\phi_t^2} \frac{g^4}{\Lambda_p} - \frac{\Lambda_p}{g^2} \right| \leq \tilde{\tau}. \quad (4.16)$$

For sake of completeness we recall that

$$\dot{\lambda}_p = -\frac{\mu_t}{6\eta_p} \left[ 1 - \frac{\tilde{\tau}}{f(\mathbf{B}_n)} \right]_+ \left( \frac{\phi_n^2}{\phi_t^2} g^4 \lambda_p^5 - \frac{1}{g^2 \lambda_p} \right), \quad (4.17)$$

and  $\lambda_p^2 \Lambda_p = 1$ .

In conclusion, one can then simplify the system (4.1) in

$$\left\{ \begin{array}{l} \frac{\partial \phi_m}{\partial t} + \frac{\partial}{\partial z} (\phi_m v_m) = 0, \\ \frac{\partial \phi_t}{\partial t} + \frac{\partial}{\partial z} (\phi_t v_t) = \Gamma_t, \\ \frac{\partial g}{\partial t} + v_t \frac{\partial g}{\partial z} = \frac{\Gamma_t}{3\phi_t} g, \\ \frac{\partial \Lambda_p}{\partial t} + v_t \frac{\partial \Lambda_p}{\partial z} = \frac{\mu_t}{3\eta_p} \left[ 1 - \frac{\tilde{\tau}}{f(\mathbf{B}_n)} \right]_+ \left( \frac{\phi_n^2}{\phi_t^2} \frac{g^4}{\Lambda_p} - \frac{\Lambda_p}{g^2} \right), \end{array} \right. \quad (4.18)$$

with

$$\left\{ \begin{array}{l} v_m = \left( K + \frac{(1 - \phi_m)^2}{\phi_m^2} K_m \right) \frac{\partial T_m}{\partial z} + \left( K - \frac{1 - \phi_m}{\phi_m} K_m \right) \frac{\partial T_t}{\partial z}, \\ v_t = \left( K - \frac{1 - \phi_m}{\phi_m} K_m \right) \frac{\partial T_m}{\partial z} + (K + K_m) \frac{\partial T_t}{\partial z}, \\ T_m = \phi_m \left( -\Sigma_m \left( \frac{\bar{\phi}_m}{\phi_m} \right) + \mu_m \frac{\bar{\phi}_m^2}{\phi_m^2} \right), \\ T_t = \phi_t \left( -\Sigma_t \left( \frac{\phi_n}{\phi_t} \right) + \mu_t \frac{\phi_n^2}{\phi_t^2} \frac{g^4}{\Lambda_p} \right). \end{array} \right. \quad (4.19)$$

In addition,

$$T_{t,rr} = \mu_t \phi_t \left( -\Sigma_t + \frac{\Lambda_p}{g^2} \right).$$

With simple modifications the same procedure illustrated above applies to the axisymmetric growth of a tumour cord around a capillary and to the spherical growth of a multicellular spheroid.

**Remark.** Plasticity implies that  $\mathbf{T}_t$  stays on the yield surface; in one-dimensional problems this condition translates into the following relationship between the strains

$$2f \left( \frac{\phi_n}{\phi_t} \frac{g^2}{\Lambda_p}, \frac{\sqrt{\Lambda_p}}{g} \right) = \tilde{\tau},$$

replacing the evolution equation for  $\Lambda_p$ . For instance, in the case  $f = f_2$ ,  $\Lambda_p$  is such that

$$\frac{1}{2} \left| \frac{\phi_n^2}{\phi_t^2} \frac{g^4}{\Lambda_p^2} - \frac{\Lambda_p}{g^2} \right| = \tilde{\tau}.$$

From the condition above one can then compute  $\Lambda_p$  in terms of  $g$ , i.e. the plastic deformation in terms of growth to remain on the yield surface.

This limit is obtained in the last equation in (4.18) for very small plastic rearrangement times, i.e.,  $\eta_p/\mu_t \ll 1$ .

## 4.2 Numerical simulations

In the simulation to follow we use a growth term similar to the one used in [16] to take contact inhibition of growth into account while neglecting the effect of nutrients and other growth factors. We will then assume that cells replicate only if the local volume ratio (or stress) is below a threshold value, otherwise they become quiescent. In addition a physiological death term is introduced so that the growth term can be modelled as

$$\Gamma_t = [\gamma H_\sigma(\bar{\phi} - \phi_t) - \delta] \phi_t \quad (4.20)$$

where  $H_\sigma$  is a regularisation of the Heaviside function of width  $\sigma$  vanishing for  $\phi_t > \bar{\phi}$ , so that  $\bar{\phi}$  is the limit value allowing proliferation. The value of  $\bar{\phi}$  referring to the tumour is slightly larger than that referring to the normal tissue, which means that tumour cells are less sensitive to mechanical cues. The stress functions  $\Sigma_m$  and  $\Sigma_t$  are modelled in the following simplest way

$$\Sigma_m = \mu_m \frac{\phi_m}{\phi_m}, \quad \Sigma_t = \mu_t \frac{\phi_t}{\phi_n}. \quad (4.21)$$

The equations are rewritten in non-dimensional form: scaling time with  $1/\gamma$  and lengths with  $\sqrt{\frac{K\mu_t}{\gamma}}$ . Considering that the elastic modulus of a soft tissue like a mammary gland is of the order of 100 Pa [38], that the permeability  $K$  is of the order of  $10^{-13} \text{ m}^2/(\text{Pa s})$  [36] and that the growth rate is of the order of one day [32, 15] then the typical time is of the order of one day and the typical length is of the order of one millimetre. We recall that  $\phi_m$ ,  $\phi_t$ ,  $g$ , and  $\Lambda_p$  are already dimensionless.

The following dimensionless numbers characterise the evolution equations

- $\tilde{K} = K_m/K$ , is the ratio between the interaction force between tumour cells and the liquid flowing around it and the one between tumour cells and the ECM. It is then expected to be one or two orders of magnitude smaller than one.
- $\tilde{\mu} = \mu_m/\mu_t$ , which refer to the ratio between the elastic moduli of the ECM and that of the ensemble of tumour cells.
- $\tilde{\tau} = \tau/\mu_t$ , is the ratio between the yield stress and the Young modulus. Since the former seems to be of the order of 1 Pa (or at most 100 Pa), this number is smaller than one.

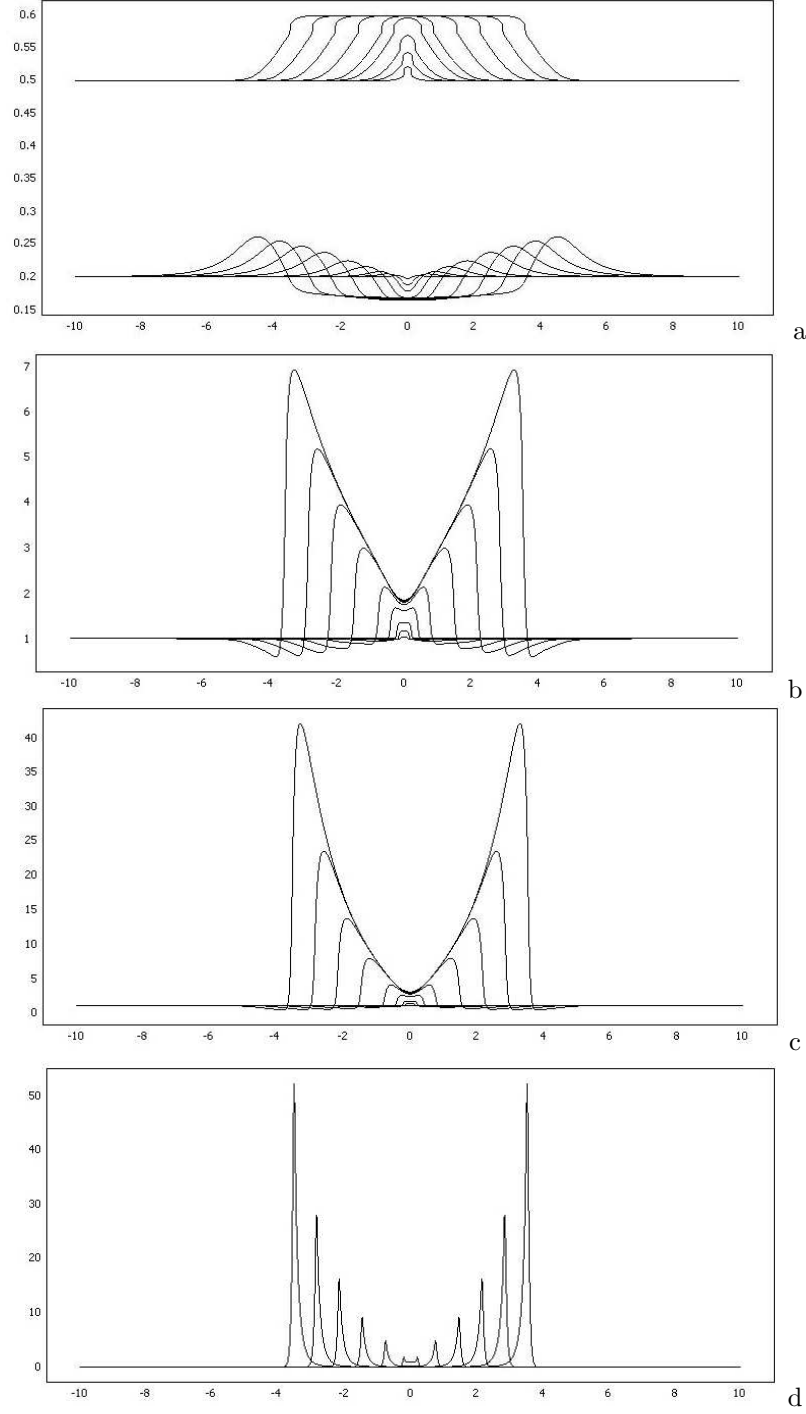


Figure 3: Tumor growth in a tissue for  $\tilde{K} = 0.1$ ,  $\tilde{\mu} = 0.1$ ,  $\tilde{\tau} = 0.01$ ,  $\tilde{\eta}_p = 0.01$ , and  $\tilde{\delta} = 0.1$  at  $\tilde{t} = 0.1, 0.5, 1, 2, 4, 8, 12, 16, 20$ . (a) Cell volume ratio (upper set of curves) and ECM volume ratio (lower set of curves) versus space. The region occupied by the tumour is the central region. Its borders can be well identified by the inflection points (points with almost vertical slopes). The outer region is occupied by the host tissue. (b) Growth. (c) Plastic deformation. (d)  $\dot{\Lambda}_p$  (only for  $\tilde{t} = 0.1, 1, 4, 8, 12, 16, 20$  for sake of clarity).

- $\tilde{\eta}_p = \nu\eta_p/\mu_t$ , is the ratio between the characteristic stress relaxation time due to cell reorganisation and the duplication time. Since the former is of the order of minutes up to few hours, it is at least an order of magnitude smaller than the characteristic time chosen on the basis of the duplication time.
- $\tilde{\delta} = \delta/\gamma$ , is the ratio between the apoptotic and the growth rate.

Equation (4.18) remain formally unchanged if space, time and velocities are considered dimensionless and  $\mu_t/\eta_p$  is replaced by  $1/\tilde{\eta}_p$ . We instead specialise Eq. (4.19) for sake of completeness (dropping tildes for the velocities and the stresses)

$$\left\{ \begin{array}{l} v_m = \left(1 + \frac{(1 - \phi_m)^2}{\phi_m^2} \tilde{K}\right) \frac{\partial T_m}{\partial z} + \left(1 - \frac{1 - \phi_m}{\phi_m} \tilde{K}\right) \frac{\partial T_t}{\partial z}, \\ v_t = \left(1 - \frac{1 - \phi_m}{\phi_m} \tilde{K}\right) \frac{\partial T_m}{\partial z} + (1 + \tilde{K}) \frac{\partial T_t}{\partial z}, \\ T_m = -\tilde{\mu}\phi_m \left(\frac{\phi_m}{\phi_m} - \frac{\phi_m^2}{\phi_m^2}\right), \\ T_t = -\phi_t \left(\frac{\phi_t}{\phi_n} - \frac{\phi_n^2}{\phi_t^2} \frac{g^4}{\Lambda_p^2}\right). \end{array} \right. \quad (4.22)$$

The values used in the following simulations are given in Table 1.

Parameter	Estimated value
$\tilde{\delta}$	0.1
$\tilde{\phi}$	0.5
$\phi_n$	0.49
$\tilde{\phi}_m$	0.2
$\tilde{K}$	0.01–0.1
$\tilde{\mu}$	0.01–0.1
$\tilde{\tau}$	0.01–0.1
$\tilde{\eta}_p$	0.01–0.1

Table 1: Parameters.

Initially a tumour is located in the interval  $x \in [-0.1, 0.1]$  and is surrounded by the host tissue. The same variables are used in the tumour and in the the host. The initial volume ratio is equal to 0.5 everywhere. In the simulations to follows the only difference between the behaviour in two regions stays in the proliferation term. In fact, similarly to what done in [16] tumour cells are assumed to be less sensitive to compression and to stop duplicating only when the volume ratio reaches  $\tilde{\phi} = 0.6$ , rather than when it reaches  $\tilde{\phi} = 0.5$ .

The general feature of the simulation is the following: initially the ensemble of tumour cells starts growing and compressing the tissue outside. Upon reaching the value of contact inhibition of the tumour, cells stop duplicating in the core of the tumour and continue duplicating close to the border, compressing more and more the tissue outside. When the compression of the surrounding tissue gets larger than that allowing duplication cells die without reproduction. At the same time, the ECM is dragged by the expanding motion of the tumour cells forming a sort of capsule at the border of the tumour.

Specifically, Figure 3a shows the volume ratio quickly increasing in the centre of the tumour ( $x = 0$ ) from the rest value for a normal tissue to the one in which also tumour cell duplication is controlled by contact inhibition. This is also evident in Figure 3b where the growth function

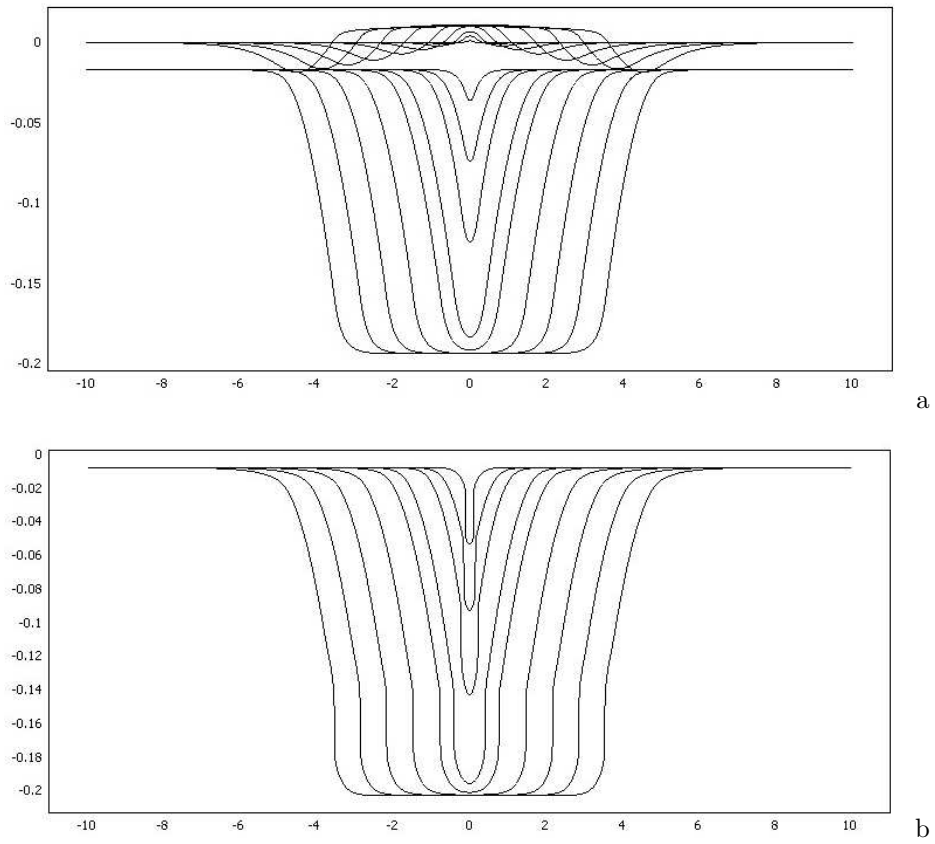


Figure 4: Stress evolution in a growing tumour for the same times and parameters as in Figure 3. (a) Axial stress related to the tumour constituent (lower set of curves) and ECM (upper set of curves) versus space. (b) Radial stress acting on the duct wall.

increases from the initial unitary value, causing a corresponding increase in  $\Lambda_p$  (Figure 3c), which measures cell reorganisation. In this set-up this is due to growth and occurs where cells are duplicating.

At about  $\tilde{t} = 2$ , the growth function  $g$  reaches in the centre a stationary value, corresponding to no net growth and therefore also no cell reorganisation. This brings to no evolution in the natural configuration in the central region and  $\Lambda_p$  and  $\phi_t$  tend there to a stationary value.

Let us turn now our attention to the interface dividing the tumour from the surrounding tissue that can be identified in Figure 3a by the strong variation in volume ratio. From the figures it can be noticed how the external tissue is compressed to volume ratios above their rest value. After  $\tilde{t} > 2$  the maximum growth (due to contact inhibition in the core of the tumour) and the maximum plastic deformations (related to cell reorganisation) occur at the tumour boundary (see Figures 3b,c,d). The region where there is evolution of the natural configuration due to plastic deformation is better put in evidence in Figure 3d.

Outside the tumour region the host tissue is compressed to a value higher than the one that can be sustained by host cells, so that they start dying, as can be deduced from Figure 3b looking at the regions where  $g < 1$ , which implies tissue resorption. This also implies  $\Lambda_p < 1$  (Figure 3c). Considering the time evolution of the volume ratio, it appears that for longer times  $\phi_t$  exhibits the profile of a travelling wave, while the components leading to the evolution of the natural configurations continue to increase with time. The dependence of the travelling wave velocity on the parameters will be examined in Figure 7.

At the same time, the extra-cellular matrix is dragged by the tumour expansion, thus forming a sort of capsule at the border of the tumour (minimum of ECM volume ratio in the centre of the tumour and maximum in the host tissue close to the boundary). No mechanisms of ECM degradation and remodelling is included in the model, so that the mass of ECM is preserved and simply displaced. For sake of clarity we remind that in reality tumour encapsulation is also due to other phenomena not considered here. For instance, a key ingredient seems to be the production of ECM at the tumour-host interface mainly by fibroblasts recruited through the chemotactic factors produced by inflammatory cells.

We observe that, as might be expected, the stiffer the ECM is (i.e., larger  $\tilde{\mu}$ ), the smaller the accumulation of ECM is at the border of the tumour (results not shown).

The time evolution of the stresses is given in Figure 4. Considering the axial components of the partial stresses represented in Figure 4a, the one referring to the tumour constituents is in compression, while the ECM is in tension inside the tumour and in compression outside it, due to the formation of the capsule, i.e. the region with higher concentration of ECM. Figure 4b instead refers to the stress that a growing tumour exerts on the duct wall.

The role of the parameters related to the description of the elasto-viscoplastic behaviours of tumours, namely  $\tilde{\tau}$  and  $\tilde{\eta}_p$  is detailed in Figures 5 and 6. In Figure 5  $\tilde{\eta}_p$  increases to 0.1 i.e., in dimensional terms, the plastic reorganisation time increases from several minutes to a few hours. As shown in Figure 5a, the evolution of cell and ECM concentration does not vary significantly: the time needed to reach in the tumour centre the growth inhibitory concentration halves, growth is a bit slower, and the “jump” near the tumour-host interface is stronger. These effects are due to the fact that cell reorganisation takes longer and consequently the stress in excess to the yield value relaxes more slowly, inhibiting growth and reducing cell motility. Coherently, Figure 5b shows that in the centre growth and plastic deformation and therefore the evolution of the natural configuration takes longer to reach the stationary value.

A stronger difference is found increasing the yield stress  $\tilde{\tau}$  to 0.1, corresponding to stronger adhesive bonds among cells. The increase in yield stress keeps the tumour more compact, which gives rise to a decrease in growth rates (see Figure 6b,c,d). The final result is a stronger decrease in the expansion velocity, which more than halves (see also Figure 7). Deformation of the ECM is much smaller, without the formation of a capsule around the tumour (see Figure 6a).

As already observed, at longer times the expansion velocity of the tumour is nearly constant, so that it is possible to evaluate the expansion velocity of the tumour boundary. Figure 7 shows how it depends on the two key parameters related to elasto-viscoplasticity, namely  $\tilde{\tau}$  and  $\tilde{\eta}_p$ . The expansion velocity decreases when the yield stress or the cell reorganisation time increase, though

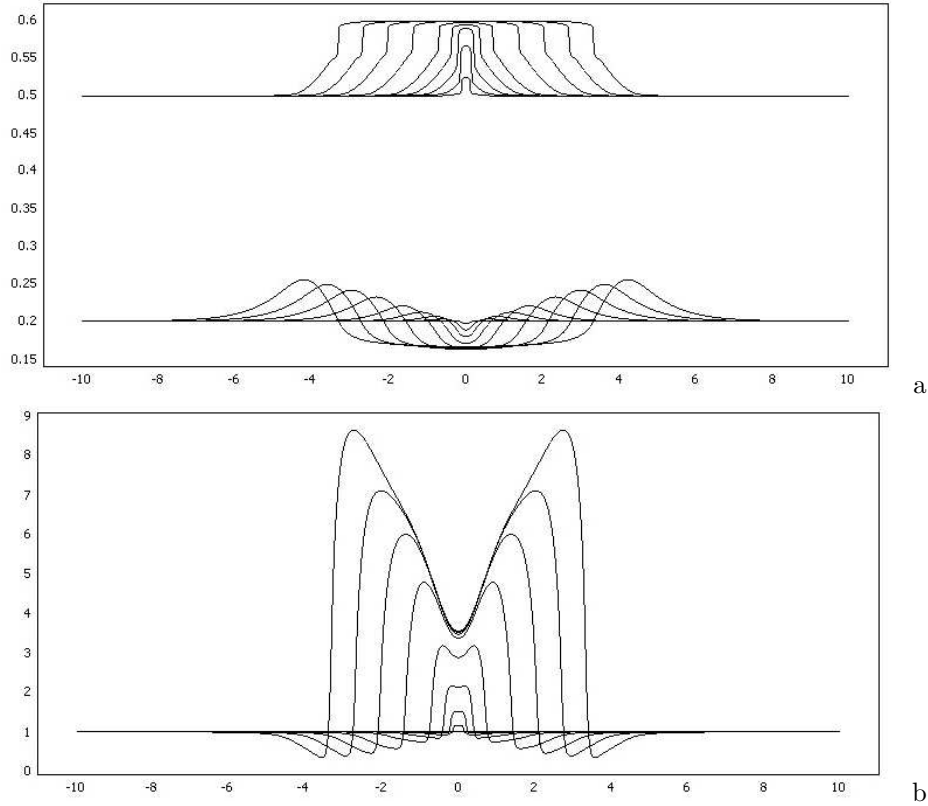


Figure 5: Tumour growth in a tissue for the same times and parameters as in Figure 3, but  $\tilde{\eta}_p$  that increases to 0.1. (a) Cell volume ratio (upper set of curves) and ECM volume ratio (lower set of curves) versus space. (b) Plastic deformation.

the dependence from the yield stress parameter is much stronger. On the other hand, we remark that the simulations performed put in evidence that the expansion velocity is almost independent from  $\tilde{K}$  or  $\tilde{\mu}$  as long as they vary in physically admissible ranges (results not shown).

## Final Remarks

The mathematical model of a solid tumour illustrated in the present paper collects a number of features that have been pointed out in the recent literature: three-dimensional formulation, use of mixture theory, stress-growth relationships, cell adhesion. Apart from the interest in a unified presentation of these aspects, the novelty of the present formulation is in its attempt to account for the mechanical behaviour of a conglomeration of cells that are weakly bounded to each other.

The reader with a background in materials science might be surprised that there is such an uncertainty on the mechanical characterisation of solid tumours, so that many more theoretical papers exist rather than experimental. As a matter of fact, experimental characterisation of tumour spheroids in a classical sense is not an easy task: they are very small (1-2 millimetres), they break out for small loads and, most important, it is quite difficult to preserve their mechanical properties during experiments maintaining a suitable environment for their survival (temperature, nutrients and so on). To our knowledge, the only relevant experiments are due to Forgacs and co-workers [19]: they load normally a cell aggregate and they measure the curvature of the free surface between the plates. Starting from the assumption that internal forces between cells are hydrostatic (pressure only), they correlate the pressure gap to the curvature radius in terms of

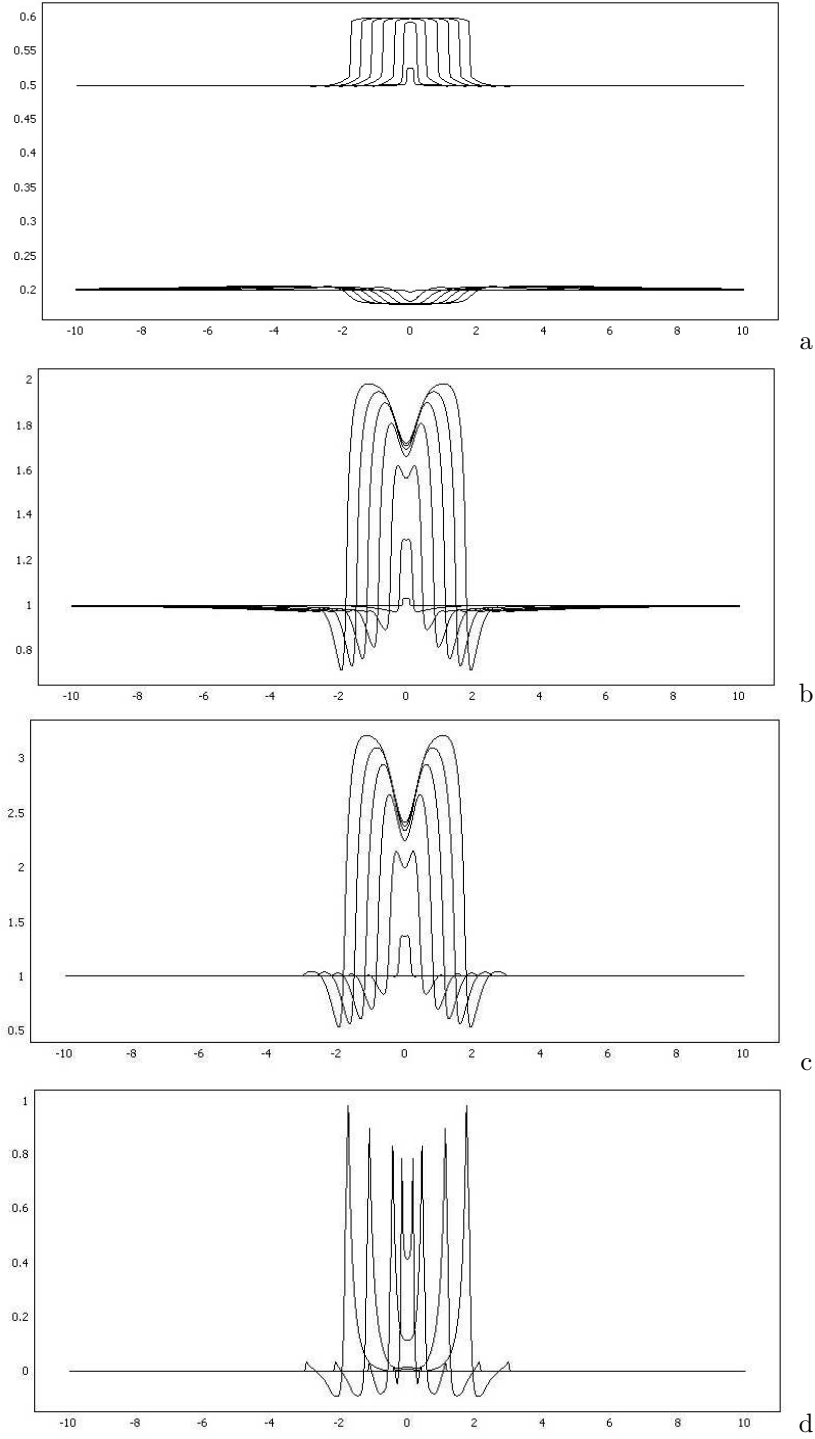


Figure 6: Tumour growth in a tissue for the same parameters as in Figure 3, but  $\tilde{\tau}$  that increases to 0.1 at  $\tilde{t} = 0.1, 1, 4, 8, 12, 16, 20$ . (a) Cell volume ratio (upper set of curves) and ECM volume ratio (lower set of curves) versus space. The region occupied by the tumour is the central region. Its borders can be well identified by the inflection points (points with almost vertical slopes). The outer region is occupied by the normal tissue. (b) Growth. (c) Plastic deformation. (d)  $\dot{\Lambda}_p$  (only for  $\tilde{t} = 0.1, 1, 4, 12, 20$  for sake of clarity).

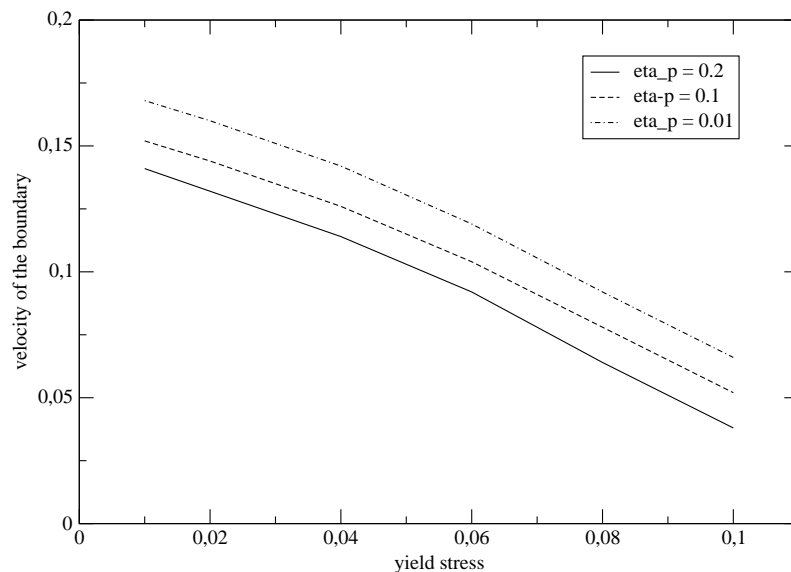


Figure 7: Velocity of the tumour border as a function of  $\tilde{\tau}$  for  $\tilde{\eta}_p = 0.01, 0.1, 0.2$ .

surface tension. A possible alternative explanation is given in [33]

Solid tumours are conventionally classified as soft tissues, but they miss some ordered components that mechanically characterise skin, arteries, veins and ligaments. Tumour matter does not include elastin and well structured collagen fibres, the constituents that make other soft tissues hyperelastic materials. In fact, a fully elastic model can yield to large unrealistic tensions in the tumour (as pointed out, for instance, by Volokh [49]). Fluid models, as the one in [19] provide a nice explanation for a normal load experiment, but they leave an open question about the behaviour of cell aggregates under shear stress: if the flow occurs for any applied load, the fluid assumption is correct. If the flow starts up just above a minimum threshold, internal forces of plastic type should be kept into account. As single cells adhere each other with a force of limited strength, we suspect that a yield stress exists to trigger cells rolling and this should be included in a macroscopic model.

The introduction of an elasto-viscoplastic constitutive law provides a mechanism for stress relaxation while preserving a precise mathematical framework to the theory. Previously proposed constitutive models are obtained as limit cases. Experiments in this direction will supply measures of yield stress and will possibly clarify under what conditions simpler models are acceptable. In this respect, in addition to uni-axial tests [8, 14, 37, 48] it would be very important to perform shear tests on multicellular spheroids, also interfering with the adhesion molecules by modifying the anchorage mechanism, or by the use of antibodies of the extracellular domain.

From the modelling viewpoint, the model proposed here can be developed further by treating in more detail the adhesion mechanisms between cells and the different constituents of the extracellular matrix. In fact, both the adhesion mechanisms involving cadherins and integrins are relevant to understand tissue invasion by the tumour.

Other developments can be obtained taking into account of several phenomena not considered here, e.g.,

- the influence of nutrients and chemical factors, such as growth promoting factors and growth inhibitory factors, both diffusible and bounded to the ECM, on growth and death;
- the consequent formation of hypoxic and necrotic regions characterised, for instance, by different adhesive properties;

- the distinction of the cellular populations in several sub-populations or clones with different adhesive characteristics;
- the presence of chemical factors influencing the transition of the cells to a mesenchymal state and therefore their motility;
- ECM remodelling through the production of matrix degrading enzymes;
- heterogeneities in the host tissue, e.g. with the presence of basal membranes, capillaries, or of other compartments.

All the problems above are of big interest and need to be developed having in mind specific tumours. In this respect, our plan is to apply the present framework to the development of pancreatic tumours.

### Acknowledgements

Partially supported by the European Community, through the Marie Curie Research Training Network Project HPRN-CT-2004-503661 “Modelling, Mathematical Methods and Computer Simulation of Tumour Growth and Therapy” and by the Italian Ministry for University and Research, through a PRIN project on “Modelli matematici di crescita e vascolarizzazione di tumori e tessuti biologici”.

### References

- [1] D. Ambrosi and F. Mollica (2002). On the mechanics of a growing tumour, *Int. J. Engng. Sci.* **40**: 1297–1316.
- [2] D. Ambrosi and F. Mollica (2004). The role of stress in the growth of a multicell spheroid, *J. Math. Biol.* **48**: 477–499.
- [3] D. Ambrosi and L. Preziosi (2002). On the closure of mass balance models for tumour growth, *Math. Mod. Meth. Appl. Sci.* **12**: 737–754.
- [4] R.P. Araujo and D.L.S. McElwain (2005). A mixture theory for the genesis of residual stresses in growing tissues, I: A general formulation, *SIAM J. Appl. Math.* **65**: 1261–1284.
- [5] R.P. Araujo and D.L.S. McElwain (2005). A mixture theory for the genesis of residual stresses in growing tissues, II: Solutions to the biphasic equations for a multicell spheroid, *SIAM J. Appl. Math.* **65**: 1285–1299.
- [6] R.P. Araujo and D.L.S. McElwain (2004). A linear-elastic model of anisotropic tumour growth, *Eur. J. Appl. Math.* **15**: 365–384.
- [7] I.V. Basov and V.V. Shelukhin (1999). Generalized solutions to the equations of compressible Bingham flows, *Z. Angew. Math. Mech.* **79**: 185–192.
- [8] W. Baumgartner, P. Hinterdorfer, W. Ness, A. Raab, D. Vestweber, H. Schindler, and D. Drenkhahn (2000). Cadherin interaction probed by atomic force microscopy, *Proc. Nat. Acad. Sci. USA* **97**: 4005–4010.
- [9] C.J.W. Breward, H.M. Byrne, and C.E. Lewis (2002). The role of cell-cell interactions in a two-phase model for avascular tumour growth, *J. Math. Biol.* **45**: 125–152.
- [10] C.J.W. Breward, H.M. Byrne, and C.E. Lewis (2003). A multiphase model describing vascular tumour growth, *Bull. Math. Biol.* **65**: 609–640.

- [11] R. Buscall, P.D.A. Mills, J.W. Goodwin, and D.W. Lawson (1988). Scaling behaviour of the rheology of aggregate networks formed from colloidal particles, *J. Chem. Soc. Faraday Trans.* **84**: 4249–4260.
- [12] H.M. Byrne, J.R. King, D.L.S. McElwain, and L. Preziosi, (2003). A two-phase model of solid tumour growth, *Appl. Math. Letters* **16**: 567–573.
- [13] H.M. Byrne and L. Preziosi (2004). Modeling solid tumour growth using the theory of mixtures, *Math. Med. Biol.* **20**: 341–366.
- [14] E. Canetta, A. Duperray, A. Leyrat and C. Verdier, (2005). Measuring cell viscoelastic properties using a force-spectrometer: Influence of the protein-cytoplasm interactions, *Biorheology* **42**: 298–303.
- [15] L. Caveda, I. Martin-Padura, P. Navarro, F. Breviario, M. Corada, D. Gulino, M.G. Lampugnani, and E. Dejana (1996). Inhibition of cultured cell growth by vascular endothelial cadherin (cadherin-5/VE-cadherin), *J. Clin. Invest.* **98**: 886–893.
- [16] M. Chaplain, L. Graziano, and L. Preziosi (2006). Mathematical modelling of the loss of tissue compression responsiveness and its role in solid tumour development, *Math. Med. Biol.* **23**: 197–229.
- [17] C.Y. Chen, H.M. Byrne and J.R. King (2001). The influence of growth-induced stress from the surrounding medium on the development of multicell spheroids, *J. Math. Biol.* **43**: 191–220.
- [18] V. Cristini, J. Lowengrub, and Q. Nie (2003). Nonlinear simulation of tumour growth, *J. Math. Biol.* **46**:191–224.
- [19] G. Forgacs, R.A. Foty, Y. Shafir, and M.S. Steinberg (1998), Viscoelastic properties of living embryonic tissues: a quantitative study, *Biophys. J.* **74**: 2227–2234.
- [20] S.J. Franks, H.M. Byrne, J.R. King, J.C.E. Underwood, and C.E. Lewis (2003). Modelling the early growth of ductal carcinoma in situ of the breast, *J. Math. Biol.* **47**: 424–452.
- [21] S.J. Franks, H.M. Byrne, H.S. Mudhar, J.C.E. Underwood, and C.E. Lewis (2003). Mathematical modelling of comedo ductal carcinoma in situ of the breast, *Math. Med. Biol.* **20**: 277–308.
- [22] S.J. Franks and J.R. King (2003). Interactions between a uniformly proliferating tumour and its surrounding. Uniform material properties, *Math. Med. Biol.* **20**: 47–89.
- [23] H. Frieboes, X. Zheng, C.-H. Sun, B. Tromberg, R. Gatenby, and V. Cristini (2006). An integrated computational/experimental model of tumour invasion, *Cancer Research* **66**:1597–1604.
- [24] R.F. Gibson (1994). **Principles of Composite Material Mechanics**, McGraw-Hill.
- [25] A.E. Green and P.M. Naghdi (1969), On basic equations for mixtures, *Quart. J. Mech. Appl. Math.*, **22**:4, 427-438.
- [26] G. Helmlinger, P.A. Netti, H.C. Lichtenbeld, R.J. Melder, and R.K. Jain (1997). Solid stress inhibits the growth of multicellular tumour spheroids, *Nature Biotech.* **15**: 778–783.
- [27] K. Hohenemser and W. Prager (1932). Über die ansätze der mechanik isotroper kontinua, *ZAMM* **12**: 216–226.
- [28] N.H. Holmes (1986). Finite deformation of soft tissue: analysis of a mixture model in uni-axial compression, *J. Biomech. Engin.*, **108**:372–381.
- [29] D.D. Joseph (1990). **Fluid Dynamics of Viscoelastic Liquids**, Springer.

- [30] A.F. Jones, H.M. Byrne, J.S. Gibson, and J.W. Dold (2000). A mathematical model of the stress induced during solid tumour growth, *J. Math. Biol.* **40**: 473–499.
- [31] S.M. Klisch and A. Hoger (2003). Volumetric growth of thermoelastic materials and mixtures, *Math. Mech. Solids* **8**: 377–402.
- [32] S. Levenberg, A. Yarden, Z. Kam, and B. Geiger (1999). p27 is involved in N-cadherin-mediated contact inhibition of cell growth and S-phase entry, *Oncogene* **18**: 869–876.
- [33] W.A. Malik, S.C. Prasad, K.R. Rajagopal, L. Preziosi. (2008). On the modelling of the viscoelastic response of embryonic tissues, *Math. Mech. Solids* **13**: 81–91.
- [34] P. Macklin and J. Lowengrub (2007). Nonlinear simulation of the effect of the microenvironment on tumour growth, *J. Theor. Biol.* **245**: 677–704.
- [35] L.E. Malvern (1969). **Introduction of the Mechanics of a Continuous Medium**, Prentice Hall Inc.
- [36] P.A. Netti and R.K. Jain (2003). Interstitial transport in solid tumours, in **Cancer Modelling and Simulation**, L. Preziosi, Ed., CRC-Press - Chapman Hall, Boca Raton.
- [37] P. Panorchan, M.S. Thompson, K.J. Davis, Y. Tseng, K. Konstantopoulos, and D. Wirtz (2006). “Single-molecule analysis of cadherin-mediated cell-cell adhesion”, *J. Cell Sci.* **119**: 66–74.
- [38] M.J. Paszek, N. Zahir, K.R. Johnson, J.N. Lakins, G.I. Rozenberg, A. Gefen, C.A. Reinhart-King, S.S. Margulies, M. Dembo, D. Boettiger, D.A. Hammer, and V. M. Weaver (2005) Tensional homeostasis and the malignant phenotype, *Cancer Cell* **8**: 241–254.
- [39] L. Preziosi (1989) On an invariance property of the solution to Stokes’ first problem for viscoelastic fluids, *J. Non-Newtonian Fluid Mech.*, **33**, 225–228.
- [40] L. Preziosi and D. D. Joseph (1987). Stokes’ first problem for viscoelastic fluids, *J. Non-Newtonian Fluid Mech.*, **25**: 239–259.
- [41] L. Preziosi and A. Tosin (2008). “Multiphase modeling of tumour growth and extracellular matrix interaction: Mathematical tools and applications”, *J. Math. Biol.* in press.
- [42] T. Roose, P. A. Netti, L. L. Munn, Y. Boucher, R. K. Jain (2003) Solid stress generated by spheroid growth estimated using a linear poroelasticity model, *Microvascular Research*, **66**: 204–212.
- [43] E.K. Rodriguez, A. Hoger and A. McCulloch, (1994) Stress dependent finite growth in soft elastic tissues, *J. Biomechanics*, **27**:455-467.
- [44] T.W. Secomb and A.W. El-Kareh (2001). A theoretical model for the elastic properties of very soft tissues, *Biorheology* **38**: 305–317.
- [45] B.R. Simon (1992). Multiphase poroelastic finite element models for soft tissue structures, *Applied Mechanics Reviews* **45**: 191–218.
- [46] V.V. Shelukhin (2002). Bingham viscoplastic as a limit of non-Newtonian fluids, *J. Math. Fluid Mech.* **4**: 109–127.
- [47] P. Snabre and P. Mills (1996). Rheology of weakly flocculated suspensions of rigid particles, *J. Phys. III France* **6**: 1811–1834.
- [48] M. Sun, J.S. Graham, B. Hegedus, F. Marga, Y. Zhang, G. Forgacs, and M. Grandbois (2005). Multiple membrane tethers probed by atomic force microscopy, *Biophys. J.* **89**: 4320–4329.

- [49] K.Y, Volokh, (2006), Stresses in growing soft tissues, *Acta Biomater.* **2**: 493–504.
- [50] K. Wilmanski (1995), Lagrangean model of two-phase porous material. *J. Non-Equilibrium Thermodyn.* **20**: 50–77.